depends on the solution of the nonlinear equation. Therefore we find it essential to compare approximations (1) and (2) directly with the existing solutions of the nonlinear Poisson–Boltzmann equation.

A numerical solution for the inner problems has been obtained by Sigal.[4] The boundary value problem was solved by a combined finite-difference Newton method and computational continuation of the solution on the parameter method. This combined method has a high computational stability. Computations were made for different coordinate systems and boundary conditions including ones with known analytical solutions. The results proved the high accuracy of the method.[4]

The subtle analytical solution provided by Levine et al.[3] is very difficult for applications as compared to the approximation through the power series (3) suggested by Oldham et al.[5] a_0 can be found by considering (3) as a transcendental equation and assuming that $\phi = \phi_2$ when $x = \chi a$.

$$\phi = \sum_{n=0}^{6} a_n x^{2n}$$

$$a_1 = 2.5 \times 10^{-1} \sinh a_0$$

$$a_2 = 1.5625 \times 10^{-2} \sinh a_0 \cosh a_0$$

$$a_3 = 4.3403 \times 10^{-4}(\sinh a_0 \cosh^2 a_0 + 2 \sinh^3 a_0)$$

$$a_4 = 6.7817 \times 10^{-6}(\sinh a_0 \cosh^3 a_0 + 17 \sinh^3 a_0 \cosh a_0)$$

$$a_5 = 6.7817 \times 10^{-8}(\sinh a_0 \cosh^4 a_0 + 123 \sinh^3 a_0 \cosh^2 a_0 + 56 \sinh^5 a_0)$$

$$a_6 = 4.70952 \times 10^{-10}(\sinh a_0 \cosh^5 a_0 + 898 \sinh^3 a_0 \cosh^3 a_0 + 1801 \sinh^5 a_0 \cosh a_0) \quad (3)$$

(3) S. Levine, J. R. Marriott, G. Neale, and N. Epstein, *J. Colloid Interface Sci.*, 52, 136 (1975).
(4) V. L. Sigal in "Poverkhnostnye javlenia v dispersnikh sistemakh", Vol. 4, "Naukova dumka", Kiev, 1975, p 262.
(5) I. B. Oldham, F. G. Young, and J. F. Osterle, *J. Colloid Sci.*, 18, 328 (1963).

TABLE I

	solution method			
χa	numerical[3]	Oldham et al.[5]	linearized equation[2]	Olivares et al.[1]
0.01	1.9999	1.9999	1.9999	1.0930
0.05	1.9977	1.9999	1.9988	1.0925
0.1	1.9909	1.9851	1.9950	1.0907
0.2	1.9647	1.9600	1.9801	1.0833
0.5	1.8050	1.8070	1.8806	1.0341
1	1.4278	1.4285	1.5797	0.8818
2	0.7652	0.7679	0.8774	0.5044
3	0.3637	0.3746	0.4098	0.2365
5	0.0667	0.0700	0.0734	0.0398
7	0.0390	0.0140	0.0119	0.0057

The solutions on the axis of the capillary ($x = 0$) obtained by the above methods are given in Table I ($\phi_2 = 2$).

Apparently, the solution of the linearized equation[2] under these conditions is not much different from the numerical solution. The approximation by power series[5] has high accuracy even with larger values of ϕ_2 but the relative error for this method grows as χa increases. This error reaches (for example, on the axis of the capillary) 15.6% when $\chi a = 2$ and $\phi_2 = 6$, nearly 24% when $\chi a = 3$, $\phi_2 = 6$, and 42.5% when $\chi a = 5$, $\phi_2 = 6$.

However, with high values of χa the exact solution approaches the one for a flat capillary which has a known analytical expression for overlapping diffuse layers.[6]

The cylindrical symmetry is significant when $\chi a \lesssim 1$ and the errors mentioned above for approximation (3) become irrelevant. The electrokinetic flow in the cylindrical capillary has a number of effects when $\chi a \lesssim 1$ as was first shown in ref 4 and proved in ref 3.

Therefore the limitations of approximations (1) and (2) as a parametrical solution for the electrokinetic flow at high zeta potential are unacceptable.

Our analysis proves that it is approximation (3) which satisfactorily fits the solution of the nonlinear Poisson–Boltzmann equation in cylindrical coordinates (the inner problem).

The approximation suggested by Olivares et al. seems to be unsatisfactory.

(6) B. Burgreen and F. R. Nakache, *J. Phys. Chem.*, 68, 1084 (1964).

Picosecond Dynamics of Twisted Internal Charge-Transfer Phenomena

Ying Wang, M. McAuliffe, F. Novak, and K. B. Eisenthal*

Department of Chemistry, Columbia University, New York, New York 10027 *(Received: July 20, 1981; In Final Form: September 4, 1981)*

We have studied the dual fluorescence of *p*-(dimethylamino)benzonitrile in propanol solution. The two emitting states were shown to reach equilibrium with an equilibration rate of 19 ± 3 ps. The forward reaction rate (20 ps) is interpreted as the time required for the molecule and solvent to relax conformationally to a charge-transfer geometry. It was also demonstrated that the short wavelength emission is from the S_1 state which is vibronically coupled to the close-lying S_2 state.

Introduction

Photoinduced charge separation is one of the most important primary processes in photochemistry and photobiology. An excited molecule can dissipate its energy through charge-transfer (CT) interactions with other ground-state molecules, leading to the formation of an exciplex or an ion pair. It can also redistribute the charges *intramolecularly* to form a large molecular dipole. Previously, we have studied[1-4] the reaction distance, the

(1) T. J. Chuang and K. B. Eisenthal, *J. Chem. Phys.*, 59, 2140 (1973); 62, 2213 (1975).

0022-3654/81/2085-3736$01.25/0

geometric requirements, and the solvent effects for the CT interaction between the anthracene (acceptor) and dimethylaniline (donor) molecules. It was found that certain geometric orientations are required to form the exciplex in nonpolar solvents whereas in highly polar solvents the exciplex reaction channel is bypassed in favor of the direct electron transfer to form an ion pair.

In this work we shall focus on the intramolecular charge redistribution process which causes the well-known anomalous dual fluorescence of *p*-(dimethylamino)benzonitrile (DMABN). In nonpolar solvents, excitation into the S_2 state of the DMABN molecule results in a single fluorescence band centered around 340 nm. However, in polar solvents a new, Stokes-shifted fluorescence appears, which is associated with a very large dipole moment of ca. 16 D.[17] A number of mechanisms have been proposed to explain the origin of this new emission band.[5-19] These include the solvent-induced level reversal of S_2 and S_1 by Lippert et al.,[5] the excimer formation by McGlynn et al.,[6-8] the excited-state proton transfer by Kosower et al.,[9,10] the complex formation with solvent by Chandross et al.,[11] and the twisted internal charge transfer by Grabowski et al.[12-17] The results accumulated over the past several years indicate that both the bond twisting (between the amino group and the benzene ring) and solvation play important roles in causing the charge redistribution.[17-19]

However, three key questions still remain to be answered. First, in spite of the numerous studies on the subject, the relationship between the two fluorescence bands is surprisingly not fully understood. The oxygen-quenching technique used by some workers[16,17] explicitly assumed the existence of an equilibrium between the two emitting states. On the other hand, direct nanosecond[20] time-resolved measurements at low temperature indicated that in MTHF solvent both fluorescence bands had rapid risetimes and long decay times, which did not support an equilibrium relationship between them. Picosecond measurements in alcohol solvents[21-24] monitored only the long wavelength emission and therefore did not provide any information on the relationship of the two bands. Our work reported here confirms the assumption made in the oxygen-quenching work. Second, the nature of the short wavelength emission band is somewhat uncertain. The S_2 and S_1 states of DMABN molecule lie close to each other (2000–4000 cm^{-1})[8,15,17] with S_2–S_0 having a much stronger transition than S_1–S_0. With excitation into the S_2 state, fluorescence polarization measurements[18] in low-temperature ethanol liquid showed mixed polarization for the short wavelength emission, having positive polarization at the low-energy side and negative polarization toward the high-energy 0–0 origin. This could be attributed to either the vibronic coupling between the emitting S_1 and the close-lying S_2 states (with mutually perpendicular transition moments) or the direct contribution of S_2 fluorescence prior to internal conversion to S_1. Our direct time-resolved data can distinguish between these two possibilities. Third, the exact role of solvent on the dynamics of the charge transfer process is still not clear. Energetically, solvation must be important, based on the facts that the dual fluorescence phenomenon was not observed in the hydrocarbon solvents, and furthermore in polar solvents the CT emission maximum Stokes shifts as the solvent polarity increases. Dynamically, several possibilities can be envisaged. For example, the photoexcited DMABN molecule could first twist, forming a strong dipole, and then be further stabilized by inducing the reorganization of the surrounding solvent molecules. This is analogous to the electron solvation phenomenon where the excess electron ejected into the liquid reorganizes the surrounding solvent molecules to form a solvated electron. It is also possible that the local solvent fluctuations couple to the conformational relaxation of the solute molecule thereby forming a favorable geometry for the CT process to occur. We intend to address the first two questions in this paper. The role of solvent is being examined and will be discussed elsewhere.

Experimental Section

A mode-locked neodymium phosphate glass oscillator generated a pulse train from which a single TEM_{00}, 4–8-ps pulse was extracted and amplified to an energy of ca. 15 mJ. The amplified 1054-nm pulse was then frequency doubled to 527 nm and frequency quadrupled to 264 nm. In this work this 264-nm pulse was used to excite the DMABN molecule and the 527-nm pulse was used both to monitor the pulse width and as a signal averaging marker. In the signal convolution procedure we have included the observed pulse broadening at 264 nm compared with that at 527 nm.

The fluorescence signal from the sample was collected and focused into an Imacon streak camera which was coupled to an OMA and interfaced to a Digital MinC computer. Fwhm of the resolution function of the streak camera–OMA system was five channels which corresponds to slightly less than 5 ps on the fastest time scale. The

(2) T. J. Chuang, R. J. Cox, and K. B. Eisenthal, *J. Am. Chem. Soc.*, **96**, 6828 (1974).
(3) Y. Wang, M. K. Crawford, and K. B. Eisenthal, *J. Phys. Chem.*, **84**, 2696 (1980).
(4) M. K. Crawford, Y. Wang, and K. B. Eisenthal, *Chem. Phys. Lett.*, **79**, 529 (1981).
(5) E. Lippert, W. Lüder, and H. Boos, *Advan. Mol. Spectrosc.*, 443 (1962).
(6) O. S. Khalil, R. H. Hofeldt, and S. P. McGlynn, *Chem. Phys. Lett.*, **19**, 479 (1972).
(7) O. S. Khalil, R. H. Hofeldt, and S. P. McGlynn, *J. Lumin.*, **6**, 229 (1973).
(8) O. S. Khalil, J. L. Meeks, and S. P. McGlynn, *Chem. Phys. Lett.*, **39**, 457 (1976).
(9) H. Dodiuk and E. M. Kosower, *Chem. Phys. Lett.*, **34**, 253 (1975).
(10) E. M. Kosower and H. Dodiuk, *J. Am. Chem. Soc.*, **98**, 924 (1976).
(11) E. A. Chandross in "The Exciplex", M. Gordon and W. R. Ware, Ed., Academic Press, New York, 1975, p 187.
(12) K. Rotkiewicz, K. H. Grellmann, and Z. R. Grabowski, *Chem. Phys. Lett.*, **19**, 315 (1973).
(13) K. Rotkiewicz and W. Rubaszenska, *Chem. Phys. Lett.*, **70**, 444 (1980).
(14) K. Rotkiewicz, Z. R. Grabowski, A. Krowczynski, and W. Kühnle, *J. Lumin.*, **12/13**, 877 (1976).
(15) J. Lipinski, H. Chojnacki, Z. R. Grabowski, and K. Rotkiewicz, *Chem. Phys. Lett.*, **58**, 379 (1978).
(16) E. Kirko-Kaminska, K. Rotkiewicz, and A. Grabowska, *Chem. Phys. Lett.*, **58**, 379 (1978).
(17) Z. R. Grabowski, K. Rotkiewicz, A. Siemiarczuk, D. J. Cowley, and W. Baumann, *Nouv. J. Chim.*, **3**, 443 (1979).
(18) W. Rettig, G. Wermuth, and E. Lippert, *Ber. Bunsenges. Phys. Chem.*, **83**, 692 (1979).
(19) W. Rettig and V. Bonačić-Koutecký, *Chem. Phys. Lett.*, **62**, 115 (1979).
(20) N. Nakashima, H. Inoue, N. Mataga, and C. Yamanaka, *Bull. Chem. Soc. Jpn.*, **46**, 2288 (1973).
(21) W. S. Struve, P. M. Rentzepis, and J. Jortner, *J. Chem. Phys.*, **59**, 5014 (1973).
(22) W. S. Struve and P. M. Rentzepis, *J. Chem. Phys.*, **60**, 1533, 1536 (1974).
(23) W. S. Struve and P. M. Rentzepis, *Chem. Phys. Lett.*, **29**, 23 (1974).
(24) W. S. Struve and P. M. Rentzepis, *J. Mol. Sci.*, **47**, 273 (1978).

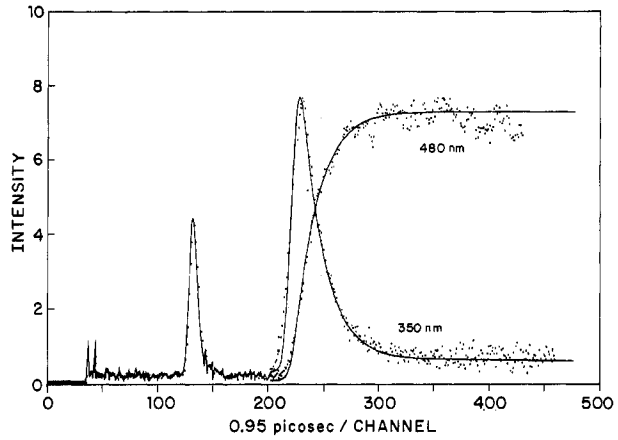

Figure 1. The DMABN fluorescence decay at 350 nm and the rise at 480 nm at fast streak speed. The solid curve is the theoretical calculation and the points are experimental data. The prepulse appearing at channel 140 is a time marker.

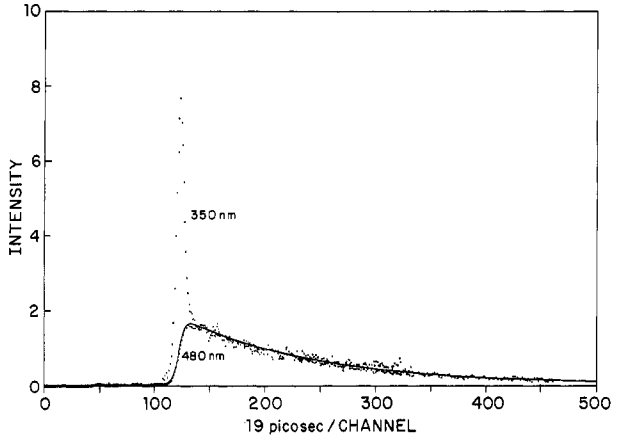

Figure 2. The DMABN fluorescence signals at 350 nm and 480 nm at slow streak speed. The solid curve is the theoretical calculation and the points are experimental data.

streak speed was calibrated with an etalon. Linearity of the intensity response was checked in every experiment and the curvature introduced by the streak camera–OMA response function was corrected for each shot.

The *p*-(dimethylamino)benzonitrile compound was purchased from Aldrich and was purified by vacuum sublimation twice. The purity was checked by NMR, absorption, and fluorescence spectra. We observed no absorption in the 330–360-nm region where an impurity had been previously observed.[25] *n*-Propyl alcohol was from Fisher (certified) and was purified by fractional distillation; it was then dried with Linde type 4A molecular sieve. All chemicals were stored in the dark, in a refrigerator, and over P_2O_5. The sample solutions were deoxygenated by repetitive freeze–pump–thaw cycles before use. All the experiments were done at 20 ± 1 °C.

Results and Discussions

We excited the DMABN molecule with a single 264-nm picosecond laser pulse. The "normal" short wavelength fluorescence and the CT fluorescence were then monitored at 350 and 480 nm, respectively, by a streak camera. The short wavelength fluorescence decay can be clearly resolved into two exponential components. The fast component decays with a lifetime of 19 ± 3 ps which is equal to the rise time of the CT fluorescence. The slow component has a lifetime of 2.3 ± 0.2 ns, which is the same as the decay of the CT emission. These results are shown in Figures 1 and 2. Care has been taken to ensure that the slow decay component at 350 nm is not due to the overlapping tail from the longer wavelength.

These results provide definitive evidence that an equilibrium is rapidly established between the states responsible for the short wavelength emission and the CT emission. This equilibrium can be described by

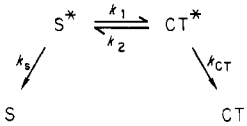

(1)

where S* represents the state responsible for the short wavelength emission, and k_S and k_{CT} represent all the other radiative and nonradiative decay rates for S* and CT*, respectively. If we assume δ-pulse excitation, the coupled differential equations can be written as

$$d[S^*]/dt = -(k_1 + k_s)[S^*] + k_2[CT^*] \quad (2)$$

$$d[CT^*]/dt = -(k_2 + k_{CT})[CT^*] + k_1[S^*] \quad (3)$$

The standard solution to the above equations are

$$I_S(t) = \frac{I_0}{\lambda_2 - \lambda_1}[(\lambda_2 - k_s - k_1)e^{-\lambda_1 t} + (k_s + k_1 - \lambda_1)e^{-\lambda_2 t}] \quad (4)$$

$$I_{CT}(t) = \frac{I_0}{\lambda_2 - \lambda_1}[e^{-\lambda_1 t} - e^{-\lambda_2 t}] \quad (5)$$

where

$$\lambda_1\ (\lambda_2) = 1/2[(k_s + k_1 + k_{CT} + k_2) \mp ((k_{CT} + k_2 - k_s - k_1)^2 + 4k_1k_2)^{1/2}] \quad (6)$$

I_S and I_{CT} are the fluorescence intensities monitored for S* and CT*, respectively. According to the above equations, the fluorescence of S* will show two exponential decays with lifetimes of $1/\lambda_1$ and $1/\lambda_2$, while the fluorescence of CT* will have an exponential rise with lifetime $1/\lambda_2$ and an exponential decay with lifetime $1/\lambda_1$. In our experiments, we measured $1/\lambda_2$ = 19 ± 3 ps and $1/\lambda_1$ = 2.3 ± 0.2 ns.

When the equilibration rate is much faster than all the other processes as in the present case, eq 6 can be further simplified to

$$\lambda_2 \simeq k_1 + k_2$$

$$\lambda_1 \simeq k_s + k_{CT}$$

Therefore the fast lifetime we measured, 19 ± 3 ps, represents the sum of the forward and backward equilibration rate, while the long lifetime, 2.3 ± 0.2 ns, represents the sum of all the other radiative and nonradiative decay channels.

We can further separate the forward and backward rate constants by the following technique. At time zero, the intensity ratio of the total short wavelength emission to its long-life component can be written as $(\lambda_2 - \lambda_1)/(\lambda_2 - k_s - k_1)$ according to eq 4. Since $\lambda_2 >> \lambda_1$ this can be further reduced to $(k_1 + k_2)/k_2$. From the 350-nm decay curve in Figure 2 we have estimated the intensity ratio at $t = 0$ to be $\simeq$30. Setting $(k_1 + k_2)/k_2 \geq 30$ we find the forward reaction to have a lifetime of about 20 ps, which we interpret to be a measure of the conformational relaxation time required for the molecule plus solvent to achieve the charge-transfer geometry.

It is worthwhile to point out that, although the difference between the emission energies is relatively large ($\simeq$

(25) N. Nakashima and N. Mataga, *Bull. Chem. Soc. Jpn.*, 46, 3016 (1973).

1 eV), the energy difference between the two emitting states could be small if there is a large energy difference between the corresponding ground states. This is supported by various calculations[15,17,19] which showed the ground-state energy of the twisted form was higher than that of the planar form by about 0.7 eV. The fast equilibration rate reported here therefore is not inconsistent with energetic considerations.

The possibility that the short wavelength emission is due to S_2 fluorescence, as suggested by other authors for a similar compound *p*-(*N*,*N*-dimethylamino)benzoic acid methyl ester,[18,19] can be eliminated for DMABN molecule based on our new findings. We have shown that the state responsible for the short wavelength emission reaches equilibrium with the CT state within 20 ps, and then both decay with a lifetime of 2.3 ns. Since this 2.3-ns lifetime includes all the radiative and nonradiative decay channels for both states other than the equilibration process, it is highly unlikely that the S_2–S_1 vibronic relaxation rate can be slower than 2.3 ns. We therefore conclude that the short wavelength emission is due to the S_1 state which borrows intensity from S_2 by vibronic coupling.

Conclusions

We have studied the dual fluorescence of DMABN molecule in propanol. The existence of an equilibrium between the emitting states, arising from different geometries, is demonstrated by our data. The sum of the forward and backward reaction rates is 19 ± 3 ps with the forward rate estimated to be 20 ps. This latter value, 20 ps, is interpreted as the time required for the molecule and solvent to relax conformationally to the twisted charge-transfer geometry. The lifetimes of both excited states after equilibration are 2.3 ± 0.2 ns.

The short wavelength emission is due to the S_1 state which is vibronically coupled to the close-lying S_2 state and is not due to direct emission from S_2.

Acknowledgment. We gratefully acknowledge the support of the Air Force Office of Scientific Research, the National Science Foundation, and the Joint Services Electronics Program (DAAG29-79-007921011).

Mass-Selective Two-Color Photoionization of Benzene Clusters

J. B. Hopkins, D. E. Powers, and R. E. Smalley*

Rice Quantum Institute and Department of Chemistry, Rice University, Houston, Texas 77001 *(Received: July 24, 1981; In Final Form: August 26, 1981)*

Using two-color mass-selective photoionization, we have obtained the $S_1 \leftarrow S_0$ excitation spectrum of the benzene dimer, trimer, and tetramer in a supersonic beam. All clusters show a weakly induced 0_0^0 band red shifted from the forbidden monomer origin by an amount which increases monotonically with cluster size. The 6_0^1 band for all clusters is split into two features corresponding to a crystal-field-induced lifting of the degeneracy of this e_{2g} benzene vibration. Exciton splitting of the 0_0^0 band in these species was found to be less than 6 cm^{-1}. The trimer and tetramer spectra show strong progressions in van der Waals modes which ultimately correspond to the optically active phonon side bands in the bulk benzene crystal. Excited-state lifetime, fluorescence quantum yield, and band profile measurements indicate the dimer rearranges from a T-shaped geometry into a sandwich excimer within several picoseconds after laser excitation from the ground T-shaped van der Waals well. This process does not occur readily in the higher clusters.

Introduction

One of the principal advantages of the newly emergent technique of resonant two-photon ionization (R2PI)[1] is the ability to produce the molecular ion without fragmentation. This mass information is particularly valuable when the spectrum to be probed is for one species in a mixture of others with similar spectral properties. Perhaps the most demanding such application of R2PI is the study of individual members of a distribution of molecular van der Waals clusters such as the benzene species discussed in this paper. Here it is particularly important that fragmentation not accompany the ionization process so that the complicated spectral features arising from higher clusters not appear as well in the spectrum of the particular cluster under study.

For ordinary molecules such as the alkylbenzenes[1a] or naphthalene,[1b] resonant two-photon ionization cleanly produces the parent ion as long as the lasers are not sufficiently intense to fragment this ion after its initial generation. This continues to be true even if the R2PI excitation reaches far above the ionization threshold to energies where ion fragmentation would be possible. Fragmentation does not occur in these cases because the geometry of the parent ion is nearly the same as that of the neutral molecule and the Franck–Condon factors for photoionization strongly favor $\Delta v = 0$ transitions. Photoionization of vibrationally cold neutrals therefore produces vibrationally cold ions which cannot fragment, and most excess energy involved in the R2PI process is taken off as translational energy of the electron.

The situation is not nearly so favorable in the case of van der Waals clusters, however. The neutral cluster is bound (at least asymptotically) by weak instantaneous dipole–induced dipole dispersion forces while the parent ion of this cluster is bound much more strongly by monopole–induced dipole forces. In this case the Franck–

(1) (a) T. G. Dietz, M. A. Duncan, M. G. Liverman, and R. E. Smalley, *J. Chem. Phys.*, **73**, 4816 (1980); (b) M. A. Duncan, T. G. Dietz, and R. E. Smalley, *ibid.*, in press; (c) M. A. Duncan, T. G. Dietz, M. G. Liverman, and R. E. Smalley, *J. Phys. Chem.*, **85**, 7 (1981); (d) T. G. Dietz, M. A. Duncan, and R. E. Smalley, *J. Chem. Phys.*, submitted for publication.

0022-3654/81/2085-3739$01.25/0